Inorg. Chem. **2007**, *46*, 9312–9322

Tuneable Intramolecular Intermetallic Interactions as a New Tool for Programming Linear Heterometallic 4f–4f Complexes

Natalia Dalla-Favera,[†] Josef Hamacek,*[,†] Michal Borkovec,[†] Damien Jeannerat,[‡] Gianfranco Ercolani,[§] and Claude Piguet*[,†]

Department of Inorganic, Analytical and Applied Chemistry, and Department of Organic Chemistry, University of Geneva, 30 quai E. Ansermet, CH-1211 Geneva 4, Switzerland. Dipartimento di Scienze e Tecnologie Chimiche, Università di Roma Tor Vergata, Via della Ricerca Scientifica, 00133 Roma, Italy

Received July 3, 2007

Statistical mechanics predicts that the design of pure organized heteropolymetallic chains of metal ions bound to linear receptors depends on controlled deviations from the mixing rule $\Delta E^{M_iM_j} = {}^1/_2\,(\Delta E^{M_iM_i} + \Delta E^{M_jM_j})$, whereby $\Delta E^{M_iM_j}$ is the intramolecular intermetallic interaction between neighboring metal i and metal j along the receptor. A thorough investigation of linear polymetallic trivalent lanthanide triple-stranded helicates shows that such deviations are amplified by an increase in the nuclearity of the final complexes and are thus easily evidenced in the tetranuclear heterobimetallic helicates $[La_{4-y}Lu_y(\mathbf{L6})_3]^{12+}$ ($y = 0$–4). The chemical and physical origins of this unprecedented behavior are discussed together with its practical consequences for programming pure heteropolymetallic 4f–4f complexes.

Introduction and Theory

Since the magnetic communication between trivalent lanthanides, Ln(III), is particularly inefficient,[1] *homo*polymetallic 4f−4f complexes have been mainly exploited for the confinement of charged,[2] noncoupled magnetically active,[3] and optically active[4] probes within a small (supra)-molecular volume. The rational preparation of organized *hetero*polymetallic lanthanide complexes is more attractive because of the novel properties emerging from the asymmetry of the intermetallic communication processes.[5] Obvious applications can be found in homogeneous fluoroimmunoassays,[6] in the combination of luminescent stains with magnetic probes for the double sensing of protein domains,[7] in the design of efficient catalysts for cleaving phosphodiester bonds,[8] and in the synthesis of materials for directional light conversion,[4,5] photonic amplification,[9] and nonlinear optical up-conversion.[10] Because of the similar coordination behavior

* To whom correspondence should be addressed. E-mail: Claude.Piguet@chiam.unige.ch (C.P.), Josef.Hamacek@chiam.unige.ch (J.H.).
† Department of Inorganic Chemistry, University of Geneva.
‡ Department of Organic Chemistry, University of Geneva.
§ Dipartimento di Scienze e Tecnologie Chimiche, Università di Roma.

(1) (a) Benelli, C.; Gatteschi, D. *Chem. Rev.* **2002**, *102*, 2369−2387. (b) Ishikawa, N.; Iino, T.; Kaizu, Y. *J. Phys. Chem. A.* **2002**, *106*, 9543−9550. (c) Ishikawa, N.; Sugita, M.; Okubo, T.; Tanaka, N.; Iino, T.; Kaizu, Y. *Inorg. Chem.* **2003**, *42*, 2440−2446. (d) Ishikawa, N.; Otsuka, S.; Kaizu, Y. *Angew. Chem., Int. Ed.* **2005**, *44*, 731−733. (e) Ishikawa, N. *Polyhedron* **2007**, *26*, 2147−2153.
(2) (a) Chawla, H. M.; Hooda, U.; Singh, V. J. *J. Chem. Soc., Chem. Commun.* **1994**, 617−618. (b) Pratviel, G.; Bernardou, J.; Meunier, B. *Adv. Inorg. Chem.* **1998**, *45*, 251−312. (c) Liu, C.; Wang, M.; Zhang, T.; Sun, H. *Coord. Chem. Rev.* **2004**, *248*, 147−168.
(3) (a) Comblin, V.; Gilsoul, D.; Hermann, M.; Humblet, V.; Jacques, V.; Mesbahi, M.; Sauvage, C.; Desreux, J. F. *Coord. Chem. Rev.* **1999**, *185*−*186*, 451−470. (b) Livramento, J. B.; Toth, E.; Sour, A.; Borel, A.; Merbach, A. E.; Ruloff, R. *Angew. Chem., Int. Ed.* **2005**, *44*, 1480−1484. (c) Costa, J.; Ruloff, R.; Burai, L.; Helm, L.; Merbach, A. E. *J. Am. Chem. Soc.* **2005**, *127*, 5147−5157. (d) Livramento, J. B.; Sour, A.; Borel, A.; Merbach, A. E.; Toth, E. *Chem.—Eur. J.* **2006**, *12*, 989−1003.
(4) (a) Bünzli, J.-C. G.; Piguet, C. *Chem. Soc. Rev.* **2005**, *34*, 1048−1077. (b) Yang, J.; Li, G.-D.; Cao, J. J.; Li, G. H.; Chen, J.-S. *Inorg. Chem.* **2007**, *45*, 2857−2865.
(5) (a) Piguet, C.; Bünzli, J.-C. G. *Chem. Soc. Rev.* **1999**, *28*, 347−358. (b) Bünzli, J.-C. G.; Piguet, C. *Chem. Rev.* **2002**, *102*, 1897−1928.
(6) Yam, V. W.-W.; Lo, K. K.-W. *Coord. Chem. Rev.* **1999**, *184*, 157−240.
(7) (a) Yu, J.; Parker, D. A.; Pal, R.; Poole, R. A.; Cann, M. J. *J. Am. Chem. Soc.* **2006**, *128*, 2294−2299. (b) Vandevyver, C. D. B.; Chauvin, A.-S.; Comby, S.; Bünzli, J.-C. G. *Chem. Commun.* **2007**, 1716−1718. (c) Martin, L. J.; Hähnke, M. J.; Wöhnert, J.; Silvaggi, N. R.; Allen, K. N.; Schwalbe, H.; Imperiali, B. *J. Am. Chem. Soc.* **2007**, *129*, 7106−7113.
(8) (a) Ragunathan, K. G.; Schneider, H.-J. *Angew. Chem., Int. Ed. Engl.* **1996**, *35*, 1219−1221. (b) Liu, C.; Wang, M.; Zhang, T.; Sun, H. *Coord. Chem. Rev.* **2004**, *248*, 147−168.
(9) (a) Oh, J. B.; Kim, Y. H.; Nah, M. K.; Kim, H. K. *J. Lumin.* **2005**, *111*, 255−264. (b) Li, L.; Jiang, W.; Pan, H.; Xu, X.; Tang, Y.; Ming, J.; Xu, Z.; Tang, R. *J. Phys. Chem. C* **2007**, *111*, 4111−4115.
(10) Auzel, F. *Chem. Rev.* **2004**, *104*, 139−173.

10.1021/ic701308h CCC: $37.00
Published on Web 10/04/2007

of the trivalent lanthanides along the 4f series, thermodynamic segregation between different metals was limited for a long period to empirical, but remarkable, deviations from pure statistical doping in solid-state materials.[11] However, the contribution of the noncontrolled crystallization processes to the latter deviations remained obscure, which limited the rational design of pure heterometallic 4f−4f to stepwise metalation/demetalation processes operating in kinetically inert lanthanide complexes with negatively charged ligands, such as porphyrin and phthalocyanin (part a of Figure 1),[12] metallocryptands,[13] and podands or macrocycles grafted with several carboxylate donors (part b of Figure 1).[14]

The recent quantitative preparation of (i) heterobimetallic binuclear $[Ln^ALn^B(\mathbf{L1}\text{-}3H)(NO_3)_2]^+$ complexes with the smallest metal occupying the internal N_4O_3 cavity (part c of Figure 1)[15] and (ii) heterobimetallic heptanuclear lanthanide complexes $[Ln^A\subset(Ln^B\mathbf{L}_2)_6]^+$ with the smallest Ln(III) located at the center of the wheel in solution[16] suggests that the thermodynamic recognition of different lanthanides may result from a judicious combination of different binding sites within a semiflexible ligand. With this idea in mind, Bünzli and co-workers designed several neutral heteroleptic bistridentate ligands derived from **L2** (part d of Figure 1), which react with stoichiometric amounts of Ln^A and Ln^B to give thermodynamic mixtures of homometallic ($[(Ln^A)_2(\mathbf{L2})_3]^{6+}$ and $[(Ln^B)_2(\mathbf{L2})_3]^{6+}$) and heterobimetallic ($[(Ln^A)(Ln^B)(\mathbf{L2})_3]^{6+}$) binuclear triple-stranded helicates (eq 1, for the sake of simplicity, the lanthanides Ln^A and Ln^B are abbreviated with A and B in the thermodynamic models).

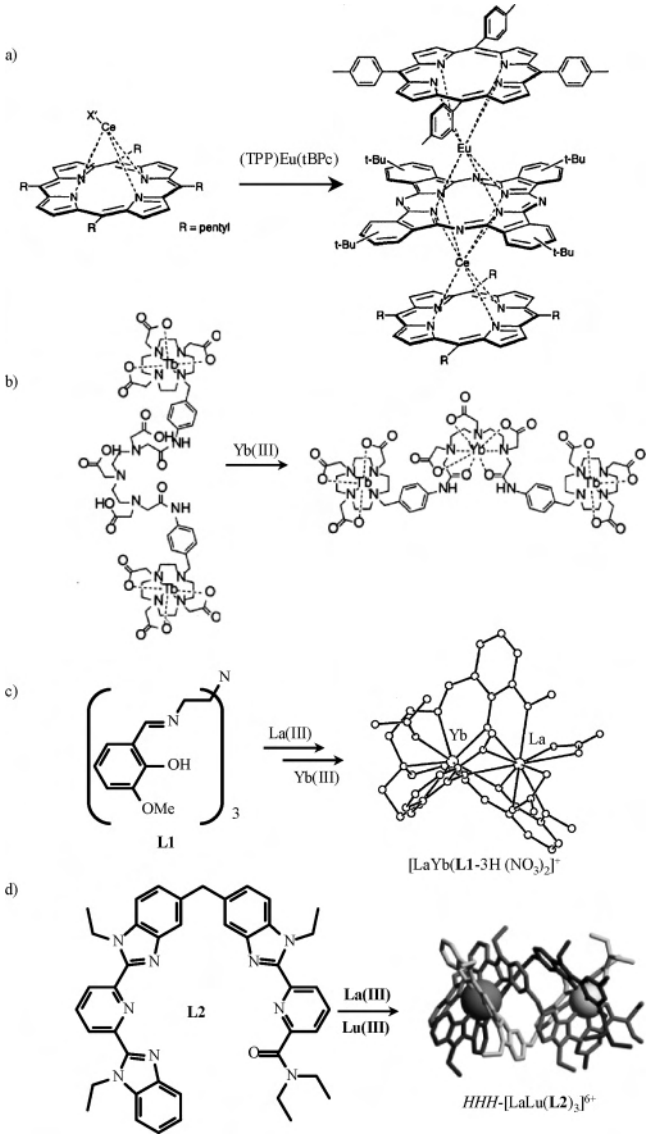

Figure 1. Selected synthetic strategies developped for designing pure heterometallic 4f−4f complexes. Kinetic control (a and b) and thermodynamic control (c and d).

$$[(Ln^A)_2(\mathbf{L}k)_3]^{6+} + [(Ln^B)_2(\mathbf{L}k)_3]^{6+} \rightleftharpoons 2[(Ln^A)(Ln^B)(\mathbf{L}k)_3]^{6+} \qquad K_{exch}^{A,B,Lk} \quad (1)$$

Interestingly, exchange equilibrium 1 is significantly shifted to the right when the difference in size between the two nine-coordinate cations $\Delta r^{LnA,LnB} = |r^{LnA} - r^{LnB}|$ increases ($K_{exch}^{Eu,Tb,L2} = 4$ for $\Delta r^{Eu,Tb} = 0.025$ Å and it reaches $K_{exch}^{La,Lu,L2} = 263$ for $\Delta r^{La,Lu} = 0.184$ Å),[17] but the rationalization of this behavior suffers from the low symmetry of the ligand **L2** (C_s symmetry), which leads to *HHH* ⇌ *HHT* structural

(11) (a) Guerriero, P.; Vigato, P. A.; Bünzli, J.-C. G.; Moret, E. *J. Chem. Soc., Dalton Trans.* **1990**, 647−655. (b) Matthews, K. D.; Fairman, R. A.; Johnson, A,; Spence, K. V. N.; Kahwa, I. A.; McPherson, G. L.; Robotham, H. *J. Chem. Soc., Dalton Trans.* **1993**, 1719−1723. (c) Froidevaux, P.; Bünzli, J.-C. G. *J. Phys. Chem.* **1994**, *98*, 532−536. (d) Bünzli, J.-C. G.; Ihringer, F. *Inorg. Chim. Acta* **1996**, *246*, 195−205. (e) Howell, R. C.; Spence, K. V. N.; Kahwa, I. A.; White, A. J. P.; Williams, D. J. *J. Chem. Soc., Dalton Trans.* **1996**, 961−968. (f) Oude Wolbers, M. P.; van Veggel, F. C. J. M.; Heeringa, R. H. M.; Hofstraat, J. W.; Geurts, F. A.; van Hummel, G. J.; Harkema, S.; Reinhoudt, D. N. *Liebigs Ann.* **1997**, 2587−2600. (g) Howell, R. C.; Spence, K. V. N.; Kahwa, I. A.; Williams, D. J. *J. Chem. Soc., Dalton Trans.* **1998**, 2727−2733. (h) Charbonnière, L. J.; Balsiger, C.; Schenk, K. J.; Bünzli, J.-C. G. *J. Chem. Soc., Dalton Trans.* **1998**, 505−510. (i) Thompson, M. K.; Vuchkov, M.; Kahwa, I. A. *Inorg. Chem.* **2001**, *40*, 4332−4341. (j) Thompson, M., K.; Lough, A. J.; White, A. J. P.; Williams, D. J.; Kahwa, I. A. *Inorg. Chem.* **2003**, *42*, 4828−4841.

(12) (a) Gross, T.; Chevalier, F.; Lindsey, J. S. *Inorg. Chem.* **2001**, *40*, 4762−4774. (b) Ishikawa, N.; Kaizu, Y. *Coord. Chem. Rev.* **2002**, *226*, 93−101. (c) Schweikart, K.-H.; Malinovskii, V. L.; Yasseri, A. A.; Li, J.; Lysenko, A. B.; Bocian, D. F.; Lindsey, J. S. *Inorg. Chem.* **2003**, *42*, 7431−7446. (d) Bian, Y.; Li, L.; Wang, D.; Choi, C.-F.; Cheng, D. Y. Y.; Zhu, P.; Li, R.; Dou, J.; Wang, R.; Pan, N.; Ng, D. K. P.; Kobayashi, N.; Jiang, J. *Eur. J. Inorg. Chem.* **2005**, *2612−2618.*

(13) Dong, Y.-B.; Wang, P.; Ma, J.-P.; Zhao, X.-X.; Wang, H.-Y.; Tang, B.; Huang, R.-Q. *J. Am. Chem. Soc.* **2007**, *129*, 4872−4873.

(14) (a) Pope, S. J. A.; Kenwright, A. M.; Heath, S. L.; Faulkner, S. *Chem. Commun.* **2003**, 1550−1551. (b) Faulkner, S.; Pope, S. J. A. *J. Am. Chem. Soc.* **2003**, *125*, 10526−10527. (c) Pope, S. J. A.; Kenwright, A. M.; Boote, V. A.; Faulkner, S. *Dalton Trans.* **2003**, 3780−3784. (d) Faulkner, S.; Burton-Pye, B. *Chem. Commun.* **2005**, 259−261. (e) Tremblay, M. S.; Sames, D. *Chem. Commun.* **2006**, 4116−4118.

(15) (a) Costes, J.-P.; Dahan, F.; Dupuis, A.; Lagrave, S.; Laurent, J.-P. *Inorg. Chem.* **1998**, *37*, 153−155. (b) Costes, J.-P.; Nicodème, F. *Chem.−Eur. J.* **2002**, *8*, 3442−3447. (c) Costes, J.-P.; Dahan, F.; Nicodème, F. *Inorg. Chem.* **2003**, *42*, 6556−6563.

(16) Chen, X.-Y.; Bretonnière, Y.; Pécaut, J.; Imbert, D.; Bünzli, J.-C. G.; Mazzanti, M. *Inorg. Chem.* **2007**, *46*, 625−637.

(17) (a) André, N.; Scopelliti, R.; Hopfgartner, G.; Piguet, C.; Bünzli, J.-C. G. *Chem. Commun.* **2002**, 214−215. (b) André, N.; Jensen, T. B.; Scopelliti, R.; Imbert, D.; Elhabiri, M.; Hopfgartner, G.; Piguet, C.; Bünzli, J.-C. G. *Inorg. Chem.* **2004**, *43*, 515−529. (c) Jensen, T. B.; Scopelliti, R.; Bünzli, J.-C. G. *Inorg. Chem.* **2006**, *45*, 7806−7814.

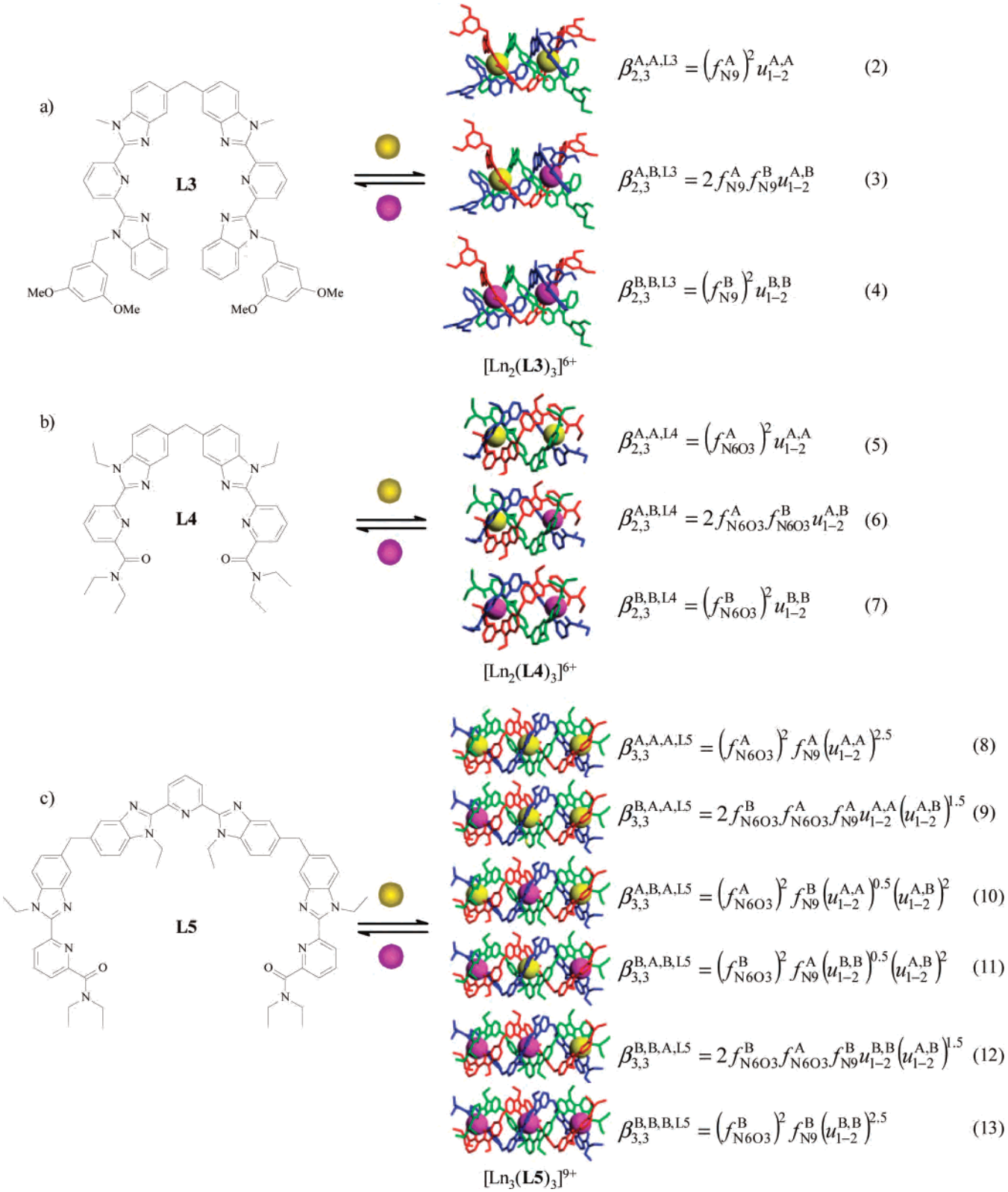

Figure 2. Self-assembly of the polynuclear triple-stranded helicates (a) $[Ln_2(\mathbf{L3})_3]^{6+}$, (b) $[Ln_2(\mathbf{L4})_3]^{6+}$, (c) $[Ln_3(\mathbf{L5})_3]^{9+}$, and the associated *site-binding* model for their formation constants (f_{N9}^{Ln} and f_{N6O3}^{Ln} are the microscopic affinities of Ln(III) for the N_9 and N_6O_3 sites, respectively, and $\Delta E_{1-2}^{Ln,Ln} = -RT\ln(u_{1-2}^{Ln,Ln})$ represents the intramolecular intermetallic interaction between two nearest neighbors).[20] The final helicates correspond to X-ray crystal structures.

isomerism (*HHH* = head-to-head-to-head, *HHT* = head-to-head-to-tail). Upon reaction of the closely related, but C_{2v}-symmetrical homotopic bis-tridentate ligands **L3** and **L4**, with a pair of lanthanides Ln^A/Ln^B, the binuclear complexes $[(Ln^A)_{2-y}(Ln^B)_y(\mathbf{Lk})_3]^{6+}$ ($y = 0-2$, $k = 3, 4$) are obtained in the absence of structural isomerism (parts a and b of Figure

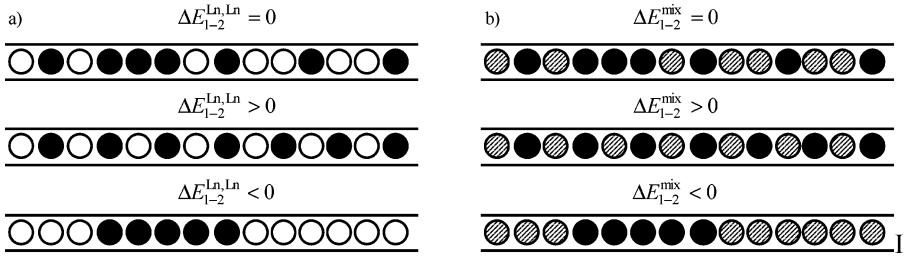

Figure 3. Pictorial representation of microstates of long linear receptors: (a) homometallic loading process and (b) heterobimetallic competition for the saturated receptor.

2).[18,19] Their associated formation constants $\beta^{A,B,Lk}_{2,3}$ can be modeled with the *site-binding* model, whereby f^{Ln}_{N9} and f^{Ln}_{N6O3} are the microscopic affinities of Ln(III) for the N9 ($[(Ln^A)_{2-y}(Ln^B)_y(\mathbf{L3})_3]^{6+}$) and N_6O_3 ($[(Ln^A)_{2-y}(Ln^B)_y(\mathbf{L4})_3]^{6+}$) sites, respectively, and $\Delta E^{Ln,Ln}_{1-2} = -RT\ln(u^{Ln,Ln}_{1-2})$ represents the intramolecular intermetallic interaction between two nearest neighbors (parts a and b of Figure 2). For the rigid assembly in question, a standard Coulombic approach predicts $\ln(u^{Ln,Ln}) \propto -\text{const}/d$, whereby d is the intermetallic distance, which eventually leads to long-range intermetallic interactions $u^{LnL,Ln}_{1-3} = (u^{Ln,Ln}_{1-2})^{0.5}$ and $u^{Ln,Ln}_{1-4} = (u^{Ln,Ln}_{1-2})^{0.33}$ because the metals are regularly spaced along the strand in **L5** and **L6** (this assumption is not critical because of the weakness of the intermetallic interaction in these complexes).[20,21]

Introducing eqs 2−4 or 5−7 in eq 1 gives eq 14, from which it is easy to deduce that any deviation from the statistical value $K^{A,B,Lk}_{exch} = 4$ ($k = 3, 4$) can be safely assigned to the deviation of the *mixing rule* controlling the intermetallic interactions $u^{mix}_{1-2} = (u^{A,A}_{1-2}u^{B,B}_{1-2})^{1/2}/u^{A,B}_{1-2} = 1$, which translates into its usual free energy formulation $\Delta E^{mix}_{1-2} = (\Delta E^{A,A}_{1-2} + \Delta E^{B,B}_{1-2})/2 - \Delta E^{A,B}_{1-2} = 0$.[20]

$$K^{A,B,Lk}_{exch} = (\beta^{A,B,Lk}_{2,3})^2/(\beta^{A,A,Lk}_{2,3}\beta^{B,B,Lk}_{2,3}) = 4(u^{A,B}_{1-2})^2/(u^{A,A}_{1-2}u^{B,B}_{1-2}) \quad (14)$$

The study of 21 different lanthanide pairs with **L4** systematically gives $K^{A,B,L4}_{exch} = 4.0(3)$, thus demonstrating that the mixing rule is obeyed for binuclear lanthanide helicates (i.e., $\Delta E^{mix}_{1-2} = 0$).[19] For the longer trinuclear helicates $[(Ln^A)_{3-y}(Ln^B)_y(\mathbf{L5})_3]^{9+}$ ($y = 0-3$), the existence of two different binding sites along the strands ($N_6O_3-N_9-N_6O_3$, in part c of Figure 2) leads to six microspecies (eqs 8−13, in part c of Figure 2), which can be combined to give the four macroconstants required for computing the relevant exchange equilibrium $K^{A,B,L5}_{exch}$ (eqs 15 and 16).[22]

$$[(Ln^A)_3(\mathbf{L5})_3]^{9+} + [(Ln^B)_3(\mathbf{L5})_3]^{9+} \rightleftharpoons [(Ln^A)_2(Ln^B)(\mathbf{L5})_3]^{9+} + [(Ln^A)(Ln^B)_2(\mathbf{L5})_3]^{9+} \quad K^{A,B,L5}_{exch} \quad (15)$$

$$K^{A,B,L5}_{exch} = \frac{(\beta^{B,A,A,L5}_{3,3} + \beta^{A,B,A,L5}_{3,3})(\beta^{B,B,A,L5}_{3,3} + \beta^{B,A,B,L5}_{3,3})}{\beta^{A,A,A,L5}_{3,3}\beta^{B,B,B,L5}_{3,3}} \quad (16)$$

(18) Piguet, C.; Bünzli, J.-C. G.; Bernardinelli, G.; Hopfgartner, G.; Williams, A. F. *J. Am. Chem. Soc.* **1993**, *115*, 8197−8206.

Table 1. Experimental Stability Constants for $[Ln_4(\mathbf{L6})_3]^{12+}$ ($\log(\beta^{Ln,L6}_{4,3,exp})$),[23] Associated Microscopic Affinities log (f^{Ln}_{N9}) and log (f^{Ln}_{N6O3}) of the N_9 and N_6O_3 Sites for Ln(III), and Intermetallic Neighboring Interactions $\Delta E^{Ln,Ln}_{1-2} = -RT\ln(u^{Ln,Ln}_{1-2})$ Obtained for the Triple-Stranded Helicates $[Ln_2(\mathbf{L3})_3]^{6+}$, $[Ln_2(\mathbf{L4})_3]^{6+}$, $[Ln_3(\mathbf{L5})_3]^{9+}$, and $[Ln_4(\mathbf{L6})_3]^{12+}$ (Simultaneous Multilinear-Least-Squares Fits of Eqs 2, 5, 8, and 17)

Ln(III)	$\log(\beta^{Ln,L6}_{4,3,exp})$	$\log(f^{Ln}_{N6O3})$	$\log(f^{Ln}_{N9})$	$\Delta E^{Ln,Ln}_{1-2}$/kJ•mol^{-1}
La	39.1(1.5)	16.9(0.7)	21.0(2.7)	48(8)
Nd	38.4(1.9)	18.8(0.9)	26.2(3.9)	67(11)
Sm	35.7(1.5)	17.1(0.3)	21.5(1.2)	48(3)
Eu	43.2(1.6)	18.7(1.4)	26.1(4.9)	67(12)
Ho	40.6(1.6)	18.4(0.9)	25.0(1.0)	62(4)
Er	38.1(1.5)	18.3(0.7)	24.2(3.0)	61(9)
Yb	41.0(1.6)	15.9(0.2)	18.2(0.9)	36(3)
Lu	40.8(1.3)	16.7(0.4)	21.1(2.0)	46(6)

The introduction of the microscopic formation constants (eqs 8−13) in eq 16 produces a complicated expression (eq S1, Supporting Information), which reduces to $K^{A,B,L5}_{exch} = 16$ under statistical conditions (i.e., $f^A_{N9} = f^B_{N9} = f^A_{N6O3} = f^B_{N6O3}$ and $u^{A,B}_{1-2} = u^{A,A}_{1-2} = u^{B,B}_{1-2}$). The detailed investigation of eight different lanthanide pairs gives $13 \le K^{A,B,L5}_{exch,exp} \le 122$, which slightly deviate from pure statistics, but closely match the exchange constants $K^{A,B,L5}_{exch,calcd}$ (eq S1) calculated with the mixing rule $\Delta E^{mix}_{1-2} = (\Delta E^{A,A}_{1-2} + \Delta E^{B,B}_{1-2})/2 - \Delta E^{A,B}_{1-2} = 0$ (Table S1, Supporting Information).[22] We can therefore assign these minor deviations from the statistics, which slightly favor the heterometallic complexes, to the different affinities of the different metals for the central (N_9) and terminal (N_6O_3) sites in the trimetallic complexes.[22] Following these experimental observations obtained for binuclear $[Ln_2(\mathbf{L3})_3]^{6+}$, $[Ln_2(\mathbf{L4})_3]^{6+}$, and trinuclear $[Ln_3(\mathbf{L5})_3]^{9+}$ helicates, the transfer matrix formalism, inherited from statisti-

(19) Zeckert, K.; Hamacek, J.; Rivera, J.-P.; Floquet, S.; Pinto, A.; Borkovec, M.; Piguet, C. *J. Am. Chem. Soc.* **2004**, *126*, 11589−11601.

(20) (a) Borkovec, M.; Hamacek, J.; Piguet, C. *Dalton Trans.* **2004**, 4096−4105. (b) Piguet, C.; Borkovec, M.; Hamacek, J.; Zeckert, K. *Coord. Chem. Rev.* **2005**, *249*, 705−726. (c) Hamacek, J.; Borkovec, M.; Piguet, C. *Dalton Trans.* **2006**, 1473−1490. (d) Borkovec, M.; Koper, G. J. M.; Piguet, C. *Curr. Opin. Colloid and Interface Sci.* **2006**, *11*, 280−289.

(21) Canard, G.; Piguet, C. *Inorg. Chem.* **2007**, *46*, 3511−3522.

(22) (a) Floquet, S.; Ouali, N.; Bocquet, B.; Bernardinelli, G.; Imbert, D.; Bünzli, J.-C. G.; Hopfgartner, G.; Piguet, C. *Chem.—Eur. J.* **2003**, *9*, 1860−1875. (b) Floquet, S.; Borkovec, M.; Bernardinelli, G.; Pinto, A.; Leuthold, L.-A.; Hopfgartner, G.; Imbert, D.; Bünzli, J.-C. G.; Piguet, C. *Chem.—Eur. J.* **2004**, *10*, 1091−1105.

(23) (a) Zeckert, K.; Hamacek, J.; Senegas, J.-M.; Dalla-Favera, N.; Floquet, S.; Bernardinelli, G.; Piguet, C. *Angew. Chem., Int. Ed.* **2005**, *44*, 7954−7958. (b) Dalla-Favera, N.; Hamacek, J.; Borkovec, M.; Jeannerat, D.; Gumy, F.; Bünzli, J.-C. G.; Ercolani, G.; Piguet, C. *Chem.—Eur. J.*, submitted.

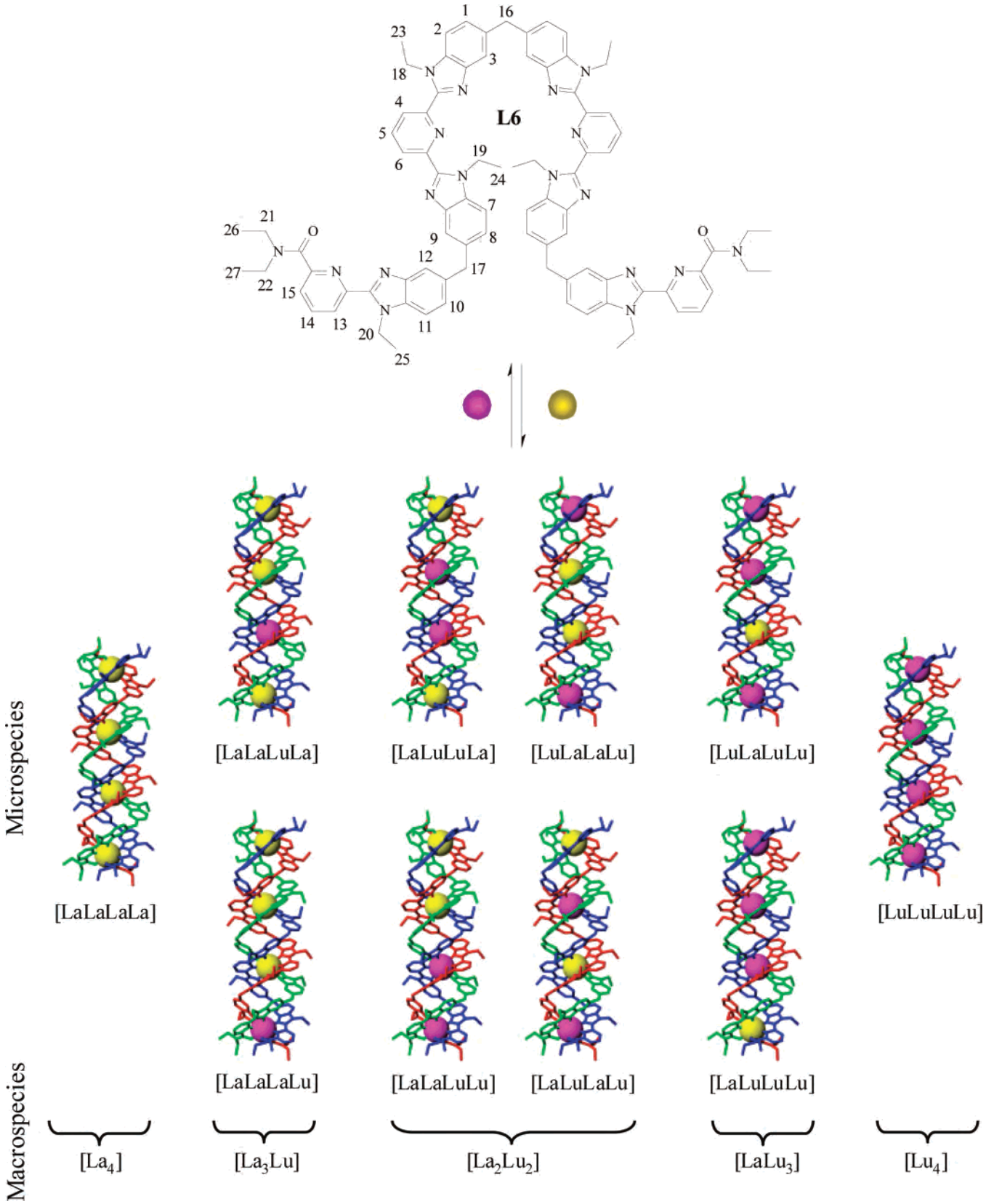

Figure 4. Self-assembly of the tetranuclear homo- and heterobimetallic triple-stranded helicates $[La_{4-y}Lu_y(\mathbf{L6})_3]^{12+}$ showing the possible micro- and macrospecies.

cal mechanics, was used to predict the partition function of infinite 1D chains of charged metals bound to a single receptor.[20] The associated binding isotherm characterizing the metal loading of the receptor strongly depends on the

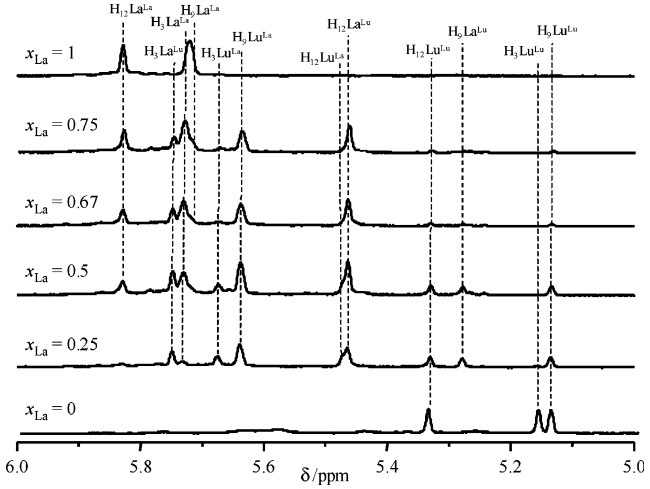

Figure 5. Experimental ^{1}H NMR spectra of H_3, H_9, and H_{12} in $[La_{4-y}Lu_y(\mathbf{L6})_3]^{12+}$ recorded for the titration of **L6** with La(III) and Lu(III) (y = 0−4, total ligand concentration = 10^{-2} M, total metal concentration = 1.33×10^{-2} M, lanthane mole fractions $x_{La} = |La|/(|La| + |Lu|) = 0-1$, CD_3CN /CD_2Cl_2 = 95:5).

nearest-neighbor pairs interaction $\Delta E_{1-2}^{Ln,Ln}$ (part a of Figure 3). Interestingly, a strict analogy exists between the latter loading process and the competition of two different metal ions A and B for saturating the linear receptor, assuming that $\Delta E_{1-2}^{Ln,Ln}$ is replaced with $\Delta E_{1-2}^{mix} = (\Delta E_{1-2}^{A,A} + \Delta E_{1-2}^{B,B})/2 - \Delta E_{1-2}^{A,B}$ (Figure 3).[20] When $\Delta E_{1-2}^{Ln,Ln} = 0$ or $\Delta E_{1-2}^{mix} = 0$, the binding sites are statistically occupied by the metals, which corresponds to non-cooperative behaviors. For the homometallic loading process (part a of Figure 3), this situation refers to a random occupancy of the metals among the binding site, whereas the related competition process produces a random distribution of the different metal ions among the coordination sites (part b of Figure 3). $\Delta E_{1-2}^{Ln,Ln} > 0$ or $\Delta E_{1-2}^{mix} > 0$ characterize anti-cooperative processes for which the repulsive interactions between the metals produce a plateau in the binding isotherm corresponding to (i) the half occupancy of the sites with strict succession of empty and occupied sites for the homometallic loading (part a of Figure 3) and (ii) a strict alternance of different metals for the heterobimetallic competition (part b of Figure 3). Finally, the (positively) cooperative processes $\Delta E_{1-2}^{Ln,Ln} < 0$ or $\Delta E_{1-2}^{mix} < 0$ result in the clustering of identical metal along the strands in both situations.

We however note that these well-defined organizations form only if $|\Delta E_{1-2}^{Ln,Ln}| \gg RT$ or $|\Delta E_{1-2}^{mix}| \gg RT$, whereby $RT \approx 2.5$ kJ·mol^{-1} at room temperature. When $|\Delta E_{1-2}^{Ln,Ln}| \ll RT$ or $|\Delta E_{1-2}^{mix}| \ll RT$, the situation is similar to a non-cooperative process, whereas $|\Delta E_{1-2}^{Ln,Ln}| \approx RT$ or $|\Delta E_{1-2}^{mix}| \approx RT$ corresponds to a transition region for which deviations from random organizations can be detected. Although such predictable programming of organized heteropolymetallic lanthanide chains is attractive for the engineering of novel materials with unusual photophysical and electronic properties,[5−10] only little attention has been focused on the tuning of intramolecular intermetallic interactions for improving complexation selectivities.[21] In this contribution, we push forward the *bottom-up* approach with the goal of inducing deviations from the statistics for the competition between

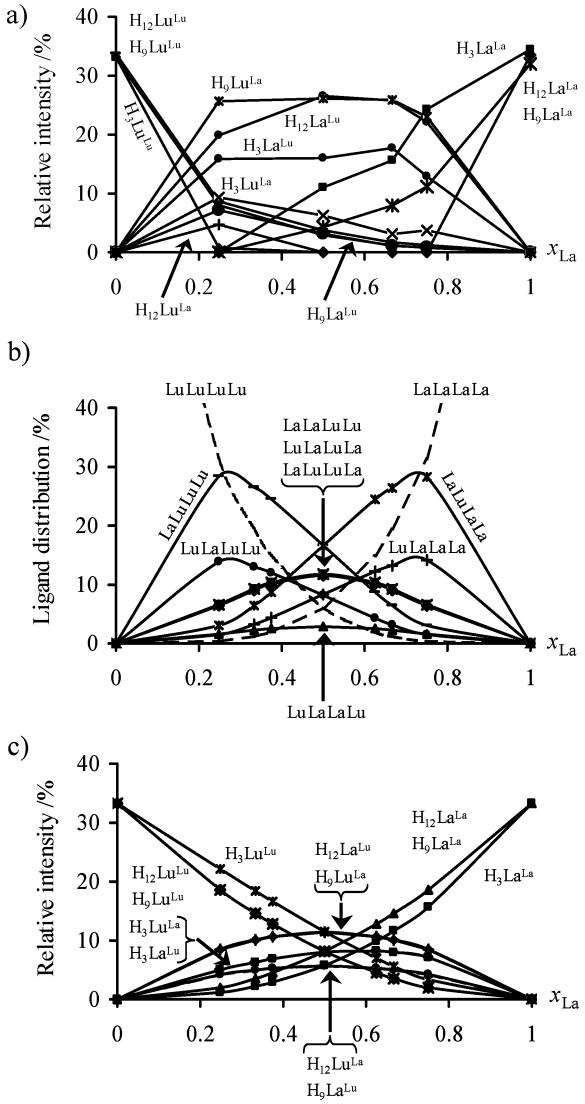

Figure 6. (a) Experimental relative intensities of ^{1}H NMR signals of protons H_3, H_9, and H_{12} in the microspecies $[La_{4-y}Lu_y(\mathbf{L6})_3]^{12+}$ obtained for the titration of **L6** with La(III) and Lu(III) (y = 0−4); (b) Simulated ligand distribution in the $[La_{4-y}Lu_y(\mathbf{L6})_3]^{12+}$ microspecies, assuming that the mixing rule is obeyed ($\Delta E_{1-2}^{mix} = 0$, Table S3); and (c) corresponding computed relative intensities of ^{1}H NMR signals of protons H_3, H_9, and H_{12} in the microspecies $[La_{4-y}Lu_y(\mathbf{L6})_3]^{12+}$ for the titration of **L6** with La(III) and Lu(III) (y = 0−4). Conditions: CD_3CN/CD_2Cl_2 = 95:5, total ligand concentration = 10^{-2} M, total metal concentration = 1.33×10^{-2} M, 298 K.

La(III) and Lu(III) in the tetranuclear helicates $[Ln_4(\mathbf{L6})_3]^{12+}$ (Figure 4).[23] Unprecedented selectivity is indeed observed, and its assignment to a combination of solvation effects, mechanical couplings, and intermetallic electrostatic interactions amplified by the nuclearity of the final (supra)molecular complexes represents a novel approach for the preparation of pure heteropolymetallic complexes and polymers.

Results and Discussion

Theoretical Model for the Metal-Exchange Process Occurring in the Tetranuclear Bimetallic Helicates $[La_{4-y}Lu_y(\mathbf{L6})_3]^{12+}$ (y = 0−4). Previous spectroscopic and thermodynamic investigations established that **L6** reacts with Ln(III) along the complete lanthanide series in acetonitrile (Ln = La−Lu, Figure 4) to give very stable tetranuclear

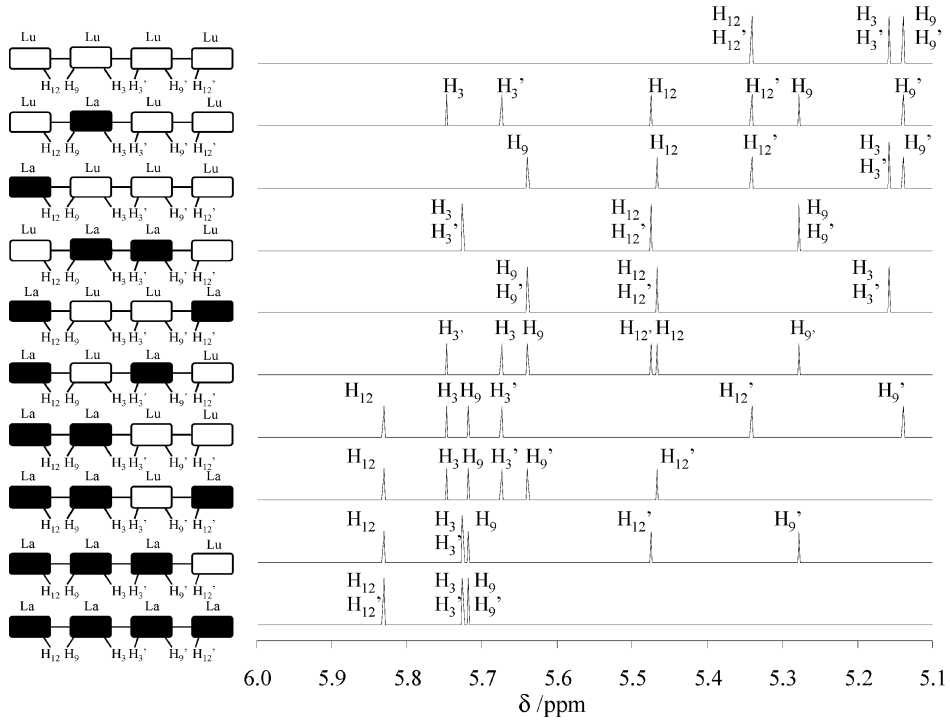

Figure 7. Individual ^{1}H NMR spectra of the 10 microspecies $[La_{4-y}Lu_y(\mathbf{L6})_3]^{12+}$ in the 5−6 ppm range ($y = 0-4$).

triple-stranded helicates $[Ln_4(\mathbf{L6})_3]^{12+}$ ($\log(\beta^{Ln,L6}_{4,3,exp})$ in Table 1, column 2).[23] This complexation process can be modeled with the *site-binding* model (eq 17),[20] and the simultaneous multilinear least-squares fit of the four formation constants previously reported for each lanthanide in the homometallic polynuclear helicates $[Ln_2(\mathbf{L3})_3]^{6+}$(eq 2 in Figure 2),[18] $[Ln_2(\mathbf{L4})_3]^{6+}$ (eq 5 in Figure 2),[19] $[Ln_3(\mathbf{L5})_3]^{9+}$ (eq 8 in Figure 2),[10] and $[Ln_4(\mathbf{L6})_3]^{12+}$ (eq 17, below)[23] provides three microscopic parameters: the microscopic affinities of Ln(III) for the N_9 and N_6O_3 sites (f^{Ln}_{N9} and f^{Ln}_{N6O3} respectively) and the intramolecular intermetallic interaction between two nearest neighbors ($\Delta E^{Ln,Ln}_{1-2} = -RT\ln(u^{Ln,Ln}_{1-2})$, Table 1, columns 3−5).

$$\beta^{A,A,A,A,L6}_{4,3} = (f^{A}_{N6O3})^2(f^{A}_{N9})^2(u^{A,A}_{1-2})^{4.33} \quad (17)$$

$$\beta^{B,A,A,A,L6}_{4,3} = 2(f^{A}_{N6O3})(f^{A}_{N9})^2(f^{B}_{N6O3})(u^{A,A}_{1-2})^{2.5}(u^{A,B}_{1-2})^{1.83} \quad (18)$$

$$\beta^{A,B,A,A,L6}_{4,3} = 2(f^{A}_{N6O3})^2(f^{A}_{N9})(f^{B}_{N9})(u^{A,A}_{1-2})^{1.83}(u^{A,B}_{1-2})^{2.5} \quad (19)$$

$$\beta^{B,A,B,A,L6}_{4,3} = 2(f^{A}_{N6O3})(f^{A}_{N9})(f^{B}_{N6O3})(f^{B}_{N9})(u^{A,A}_{1-2})^{0.5}(u^{A,B}_{1-2})^{3.33}(u^{B,B}_{1-2})^{0.5} \quad (20)$$

$$\beta^{B,B,A,A,L6}_{4,3} = 2(f^{A}_{N6O3})(f^{A}_{N9})(f^{B}_{N6O3})(f^{B}_{N9})(u^{A,A}_{1-2})(u^{A,B}_{1-2})^{2.33}(u^{B,B}_{1-2}) \quad (21)$$

$$\beta^{A,B,B,A,L6}_{4,3} = (f^{A}_{N6O3})^2(f^{B}_{N9})^2(u^{A,A}_{1-2})^{0.33}(u^{A,B}_{1-2})^{3}(u^{B,B}_{1-2}) \quad (22)$$

$$\beta^{B,A,A,B,L6}_{4,3} = (f^{B}_{N6O3})^2(f^{A}_{N9})^2(u^{A,A}_{1-2})(u^{A,B}_{1-2})^{3}(u^{B,B}_{1-2})^{0.33} \quad (23)$$

$$\beta^{A,B,B,B,L6}_{4,3} = 2(f^{B}_{N6O3})(f^{B}_{N9})^2(f^{A}_{N6O3})(u^{B,B}_{1-2})^{2.5}(u^{A,B}_{1-2})^{1.83} \quad (24)$$

$$\beta^{B,A,B,B,L6}_{4,3} = 2(f^{B}_{N6O3})^2(f^{A}_{N9})(f^{B}_{N9})(u^{B,B}_{1-2})^{1.83}(u^{A,B}_{1-2})^{2.5} \quad (25)$$

$$\beta^{B,B,B,B,L6}_{4,3} = (f^{B}_{N6O3})^2(f^{B}_{N9})^2(u^{B,B}_{1-2})^{4.33} \quad (26)$$

When the total ligand concentration is large enough ($\geq 10^{-2}$ M) to ensure the quantitative formation of $[Ln_4(\mathbf{L6})_3]^{12+}$ under stoichiometric conditions (i.e., $Ln_{tot}/\mathbf{L6} = 4:3$), the competition between the two metal ions, such as La(III) and Lu(III), simply corresponds to the intermolecular metal exchange between the saturated trigonal helicates $[La_{4-y}Lu_y(\mathbf{L6})_3]^{12+}$ ($y = 0-4$, Figure 4).

Investigation of the Experimental Metal-Exchange Process Occurring in the Tetranuclear Bimetallic Helicates $[La_{4-y}Lu_y(\mathbf{L6})_3]^{12+}$ ($y = 0-4$). The detailed ^{1}H NMR analysis (COSY, NOESY, ROESY) of the homometallic tetranuclear complexes $[La_4(\mathbf{L6})_3]^{12+}$ (part a of Figure S1, Supporting Information)[23] and $[Lu_4(\mathbf{L6})_3]^{12+}$ (part b of Figure S1, Supporting Information)[23] allows the complete assignment of the 39 signals (numbering in Figure 4). Let us now focus on the unusually shielded aromatic protons H_3, H_9, and H_{12}, which are put in the diamagnetic shielding region of a neighboring strand by the wrapping of the ligands ($\delta_H = 5.0-6.0$ ppm, Figure 5 and Figure S2, Supporting Information).[24] If all 10 $[La_{4-y}Lu_y(\mathbf{L6})_3]^{12+}$ microspecies provided a specific set of chemical environments for the protons H_3, H_9, and H_{12}, we would expect the detection of 48 different ^{1}H NMR signals. However, the stepwise transformation of $[Lu_4(\mathbf{L6})_3]^{12+}$ into $[La_4(\mathbf{L6})_3]^{12+}$ displays only 12 resolved ^{1}H NMR signals arising from H_3, H_9, and H_{12} (Figure 5), whose evolution during the titration of **L6** with La(III) and Lu(III) is shown in part a of Figure 6.

The spectral overlap can be rationalized by using a simple structural model, in which the chemical shift of each aromatic proton H_iLn1^{Ln2} ($i = 3$, 9, 12) depends only on (1) the lanthanide coordinated to the incriminated benzimidazole rings (Ln1) and (2) the lanthanide bound to the closest

neighboring site (Ln2). In these conditions, we indeed expect only 12 different ^{1}H NMR chemical environments (Table S2, Supporting Information), whose unambigous assignment to H_3, H_9, and H_{12} in the different microspecies relies on simulated intensities assuming that the mixing rule $\Delta E_{1-2}^{mix} = (\Delta E_{1-2}^{A,A} + \Delta E_{1-2}^{B,B})/2 - \Delta E_{1-2}^{A,B} = 0$ is obeyed.

We thus first calculate the distribution of the saturated bimetallic tetranuclear complexes $[La_{4-y}Lu_y(\mathbf{L6})_3]^{12+}$ by using the formation constants of eqs 17−26 with $\Delta E_{1-2}^{mix} = 0$ ($y = 0-4$, Table S3, Supporting Information). Second, the resulting predicted ligand distribution (part b of Figure 6) is combined with the intensity of each proton in each microspecies (Table S2) to give the simulated evolution of the 12 ^{1}H NMR signals for the titration of **L6** with La(III) and Lu(III) in part c of Figure 6. Comparison between the integrated experimental (part a of Figure 6) and simulated (part c of Figure 6) ^{1}H NMR signals for H_3, H_9, and H_{12} shows sufficient analogies for allowing a detailed assignment of all of the H_iLn1^{Ln2} protons (Figures 5 and 6 and Table S4). Obviously, the reconstructed individual ^{1}H NMR spectra of the 10 $[La_{4-y}Lu_y(\mathbf{L6})_3]^{12+}$ microspecies (Figure 7) display strong correlations, and factor analysis[25] indicates that only 5 spectra are mathematically independent.

Quantitative Analysis of the Experimental Metal-Exchange Process Occurring in the Tetranuclear Bimetallic Helicates $[La_{4-y}Lu_y(\mathbf{L6})_3]^{12+}$ ($y = 0-4$). Taking into account the correlation between the experimental ^{1}H NMR spectra of the microspecies (Figure 7), we limited the eventual estimation of the experimental concentrations of the bimetallic complexes in the mixtures to the five macrospecies $[La_{4-y}Lu_y(\mathbf{L6})_3]^{12+}$ ($y = 0-4$) for each different La/Lu ratio. The associated mole fractions of each macrospecies y, given as z_y, with respect to the total concentration of tetranuclear helicates are given in eqs 27−31, assuming that the relative contributions of the different microspecies within a given macrospecies is a priori fixed by the ratio of the microconstants calculated with $\Delta E_{1-2}^{mix} = 0$ (Table S3).

$$z_0 = |La_4| = |LaLaLaLa| \quad (27)$$

$$z_1 = |La_3Lu| = 0.33|LaLaLaLu| + 0.67|LaLaLuLa| \quad (28)$$

$$z_2 = |La_2Lu_2| = 0.31|LaLaLuLu| + 0.30|LaLuLaLu| + 0.31|LaLuLuLa| + 0.08|LuLaLaLu| \quad (29)$$

$$z_3 = |LaLu_3| = 0.67|LuLuLuLa| + 0.33|LuLuLaLu| \quad (30)$$

$$z_4 = |Lu_4| = |LuLuLuLu| \quad (31)$$

The total intensity of the protons can be then easily modeled by combining the individual spectra of Figure 7 with the mole fractions expressed in eqs 27−31 to give a set of 12 equations summarized in Table S5 (eqs S2−S13, Supporting Information). Multilinear least-squares fits of these equations to the experimental intensities for each La/Lu ratio (Table S4, Supporting Information) provides an estimate of the experimental concentrations z_y of the five $[La_{4-y}Lu_y(\mathbf{L6})_3]^{12+}$ ($y = 0-4$) macrospecies (part a of Figure 8). Comparison of the latter experimental distribution of the macrospecies (part a of Figure 8), with the one predicted with $\Delta E_{1-2}^{mix} = 0$ (part b of Figure 8), shows systematic deviations favoring the formation of the heterobimetallic complexes. Because the absolute affinities of the N_6O_3 and N_9 sites for La(III) and Lu(III) are very similar ($f_{N6O3}^{La} \cong f_{N6O3}^{Lu}$ and $f_{N9}^{La} \cong f_{N9}^{Lu}$, Table 1), we can rule out a selective distribution of the lanthanides in the different sites based on specific metal−ligand recognition events. We can safely conclude that the mixing rule is not obeyed and $\Delta E_{1-2}^{mix} = (\Delta E_{1-2}^{Lu,Lu} + \Delta E_{1-2}^{La,La})/2 - \Delta E_{1-2}^{La,Lu} > 0$, which is diagnostic for an anticooperative process (part b of Figure 3).[20] Consequently, the intermetallic repulsion between identical neighbors is larger that that operating between different metals. This thermodynamic deviation from statistics is in line with the experimental strong preference exhibited by the heterotopic bis-tridentate ligand **L2** for producing heterometallic $[LaLu(\mathbf{L2})_3]^{6+}$ complexes,[17] but we cannot invoke here any subtle driving forces resulting from specific interligand interactions varying with the relative orientations of the ligand strands because **L6** (C_{2v} point group) is homotopic, whereas **L2** (C_s point group) is heterotopic.

Two possible origins can be considered for rationalizing this deviation. First, the mechanical coupling between adjacent coordination sites may favor the formation of heterometallic neighboring pairs for steric (i.e., enthalpic) reasons. However, the observation that deviations from the mixing rule increase stepwise when going from the binuclear $[Ln_2(\mathbf{Lk})_3]^{6+}$ ($k = 3$, 4, the mixing rule is obeyed),[18,19] to

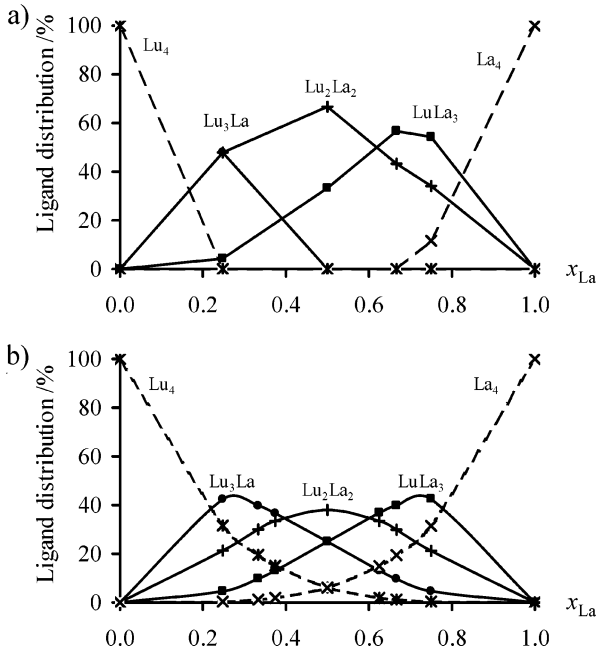

Figure 8. (a) Experimental and (b) predicted ($\Delta E_{1-2}^{mix} = 0$) ligand distributions in the macrospecies $[La_{4-y}Lu_y(\mathbf{L6})_3]^{12+}$ during the titration of **L6** with La(III) and Lu(III) ($y = 0-4$, total ligand concentration $= 10^{-2}$ M, total metal concentration $= 1.33 \times 10^{-2}$ M, lanthane mole fractions $x_{La} = |La|/(|La| + |Lu|) = 0-1$).

(24) (a) Piguet, C.; Rivara-Minten, E.; Hopfgartner, G.; Bünzli, J.-C. G. *Helv. Chim. Acta* **1995**, *78*, 1541−1566. (b) Piguet, C.; Bünzli, J.-C. G.; Bernardinelli, G.; Hopfgartner, G.; Petoud, S.; Schaad, O. *J. Am. Chem. Soc.* **1996**, *118*, 6681−6697.

(25) Malinowski, E. R.; Howery, D. G. *Factor Analysis in Chemistry*; Wiley & Sons: New York, Chichester, 1980.

Table 2. Experimental (log ($\beta_{4,3,exp}^{La(4-y)Luy,L6}$)) and Calculated (log ($\beta_{4,3,calcd}^{La(4-y)Luy,L6}$)) Formation Constants for the Macrospecies $[La_{4-y}Lu_y(\mathbf{L6})_3]^{12+}$ (Acetonitrile/dichloromethane = 95:5, 298 K)

macrospecies	log ($\beta_{4,3,exp}^{La(4-y)Luy,L6}$)	log($\beta_{4,3,calcd}^{La(4-y)Luy,L6}$) $\Delta E_{1-2}^{mix} = 0$ /kJ·mol^{-1}	log($\beta_{4,3,calcd}^{La(4-y)Luy,L6}$) $\Delta E_{1-2}^{mix} = 2$ /kJ·mol^{-1}
La_4	39.4	39.4	39.3
La_3Lu	41.0	40.3	41.1
La_2Lu_2	41.8	40.9	41.8
$LaLu_3$	41.5	41.0	41.4
Lu_4	40.6	40.7	40.6
log($K_{exch}^{La,Lu,L6}$)	8.5	4.3	8.7

the trinuclear $[Ln_3(\mathbf{L5})_3]^{9+}$ (slight deviations from the mixing rule, often difficult to address),[22] to the tetranuclear $[Ln_4(\mathbf{L6})_3]^{12+}$ helicates (significant deviations from the mixing rule) is difficult to correlate with a simple short-range mechanical coupling. The second possible explanation involves the formation of irregular helices when metal ions of different sizes are incorporated. Because we have shown that solvation effects are crucial in controlling apparent intermetallic interactions in solution,[21] a slight change in the total solvation energy of one complex in equilibrium 32 is expected to have drastic effect on the associated exchange constant $K_{exch}^{La,Lu,L6}$ (eq 33). This effect is expected to increase with the nuclearity of the complex, that is, with the total charge q borne by the helicate because the solvation energies $\Delta_{solv}G \propto q^2$ according to the Born equation.[21]

$$3[La_4(\mathbf{L6})_3]^{12+} + 3[Lu_4(\mathbf{L6})_3]^{12+} \rightleftharpoons 2[La_3Lu(\mathbf{L6})_3]^{12+} + 2[La_2Lu_2(\mathbf{L6})_3]^{12+} + 2[LaLu_3(\mathbf{L6})_3]^{12+} \quad (32)$$

$$K_{exch}^{La,Lu,L6} = (\beta_{4,3}^{La3Lu,L6}\beta_{4,3}^{La2Lu2,L6}\beta_{4,3}^{LaLu3,L6})^2/(\beta_{4,3}^{La4,L6}\beta_{4,3}^{Lu4,L6})^3 \quad (33)$$

For the pure statistical situation, $f_{N6O3}^{La} = f_{N6O3}^{Lu} = f_{N9}^{La} = f_{N9}^{Lu}$ and $\Delta E_{1-2}^{La,Lu} = \Delta E_{1-2}^{La,La} = \Delta E_{1-2}^{Lu,Lu}$, the introduction of eqs 17−26 into eq 33 predicts $K_{exch,stat}^{La,Lu,L6} = (4\cdot6\cdot4)^2 = 9216$, which can be compared with the value $K_{exch,mixingrule}^{La,Lu,L6} = 25\,119$, computed with eq 33 (Table 2, column 3) and by using the formation constants obeying the mixing rule $\Delta E_{1-2}^{mix} = (\Delta E_{1-2}^{Lu,Lu} + \Delta E_{1-2}^{La,La})/2 - \Delta E_{1-2}^{La,Lu} = 0$ (Table S3, Supporting Information). The latter value indicates that the slight differences in the absolute affinities of La(III) and Lu(III) for the terminal (N_6O_3) and central (N_9) binding site in the tetranuclear helicates $[Lu_4(\mathbf{L6})_3]^{12+}$ is responsible for a limited increase of $K_{exch}^{La,Lu,L6}$ by a factor of 25 119:9216 = 2.8. Despite the significant uncertainties affecting the experimental concentrations of the heterobimetallic macrospecies due to the limited accuracy of the integration of original correlated ^{1}H NMR signals, we have performed a nonlinear least-square fit of these concentrations (part a of Figure 8) by using the macroscopic equilibria eqs 34−38, and we obtain a set of experimental macroconstants $\beta_{4,3,exp}^{La(4-y)Luy,L6}$ (Table 2, column 2), which satisfyingly reproduces the experimental data (Figure S3, Supporting Information, Agreement factor $AF = \sqrt{\sum_i(|Conc|_{exp} - |Conc|_{calcd})^2/\sum_i(|Conc|_{exp})^2} = 0.24$, Conc = concentration).

$$4\,La^{3+} + 3\,\mathbf{L6} \rightleftharpoons [La_4(\mathbf{L6})_3]^{12+}\ \beta_{4,3}^{La4,L6} \quad (34)$$

$$3\,La^{3+} + Lu^{3+} + 3\,\mathbf{L6} \rightleftharpoons [La_3Lu(\mathbf{L6})_3]^{12+}\ \beta_{4,3}^{La3Lu,L6} \quad (35)$$

$$2\,La^{3+} + 2\,Lu^{3+} + 3\,\mathbf{L6} \rightleftharpoons [La_2Lu_2(\mathbf{L6})_3]^{12+}\ \beta_{4,3}^{La2Lu2,L6} \quad (36)$$

$$La^{3+} + 3\,Lu^{3+} + 3\,\mathbf{L6} \rightleftharpoons [LaLu_3(\mathbf{L6})_3]^{12+}\ \beta_{4,3}^{LaLu3,L6} \quad (37)$$

$$4\,Lu^{3+} + 3\,\mathbf{L6} \rightleftharpoons [Lu_4(\mathbf{L6})_3]^{12+}\ \beta_{4,3}^{Lu4,L6} \quad (38)$$

The introduction of $\beta_{4,3,exp}^{La(4-y)Luy,L6}$ in eq 33 gives $K_{exch,exp}^{La,Lu,L6} = 10^{8.5}$, which indeed corresponds to a further increase by more than 4 orders of magnitude (Table 2, column 2) of the exchange constant in favor of the heterometallic helicates. The latter effect can be thus unambigously assigned to a deviation of the mixing rule. Nonlinear least-square fits of the five constants $\beta_{4,3,exp}^{La(4-y)Luy,L6}$ to the *site binding* model (eqs 17−26), for which f_{N6O3}^{La}, f_{N6O3}^{Lu}, f_{N9}^{La}, f_{N9}^{Lu}, $\Delta E_{1-2}^{La,La}$, and $\Delta E_{1-2}^{Lu,Lu}$ were fixed (Table 1), eventually gives $\Delta E_{1-2}^{La,Lu} = 45.4$ kJ·mol^{-1} as the single fitted parameter, in agreement with an anti-cooperative mixing factor of $\Delta E_{1-2}^{mix} = (\Delta E_{1-2}^{Lu,Lu} + \Delta E_{1-2}^{La,La})/2 - \Delta E_{1-2}^{La,Lu} \approx +2$ kJ·mol^{-1} (Table 2). The agreement of the recalculated formation constants (Table 2, column 4) with the experimental data (Table 2, column 2) is excellent, and we conclude that a minor deviation from the mixing rule induces a drastic effect in the polynuclear linear chain of metal ions because of the increasing amount of intermetallic interactions accompanying the increase in nuclearity of the (supra)molecular objects. The calculation of partial occupancy factors $r_{(\mathbf{L6})_3}^{Lnj}$ introduced by Hamaceck et al.[26] for the fixation of either La(III) or Lu(III) to the virtually preorganized receptor $(\mathbf{L6})_3$ (eqs 39−40) provides globally upward convex Scatchard-like plots,[26] which are diagnostic for anti-cooperative mechanisms accompanying the successive introduction of similar metal ions within the tetranuclear helicates $[La_{4-y}Lu_y(\mathbf{L6})_3]^{12+}$ (part a of Figure 9). We can thus predict that $[La_2Lu_2]$ is the thermodynamically favored heterobimetallic macrospecies, in agreement with the computed experimental distribution curves (part b of Figure 9).

$$r_{(\mathbf{L6})_3}^{La} = \frac{|La|_{bound}}{|(\mathbf{L6})_3|_{tot}} = \frac{4|La_4| + 3|La_3Lu| + 2|La_2Lu_2| + |LaLu_3|}{|(\mathbf{L6})_3| + |La_4| + |La_3Lu| + |La_2Lu_2| + |LaLu_3| + |Lu_4|} \quad (39)$$

$$r_{(\mathbf{L6})_3}^{Lu} = \frac{|Lu|_{bound}}{|(\mathbf{L6})_3|_{tot}} = \frac{4|Lu_4| + 3|Lu_3La| + 2|La_2Lu_2| + |LuLa_3|}{|(\mathbf{L6})_3| + |La_4| + |La_3Lu| + |La_2Lu_2| + |LaLu_3| + |Lu_4|} \quad (40)$$

A close scrutiny of these Scatchard-like plots indicates that

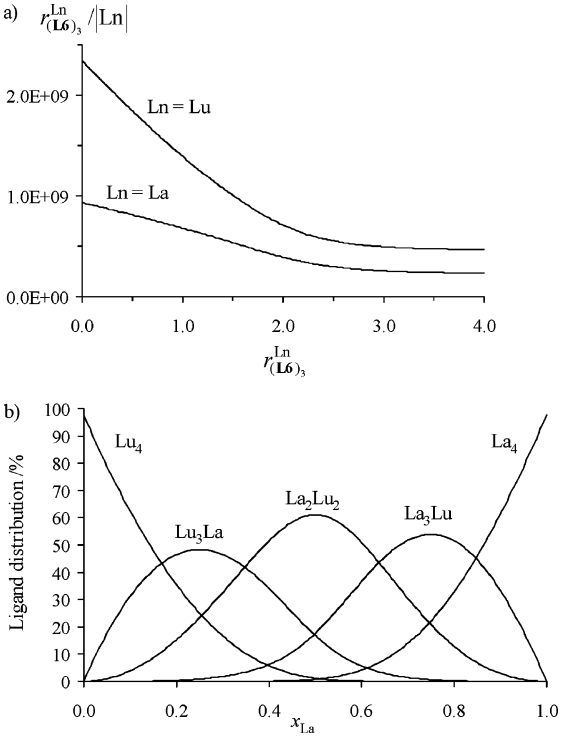

Figure 9. Experimental (a) Scatchard-like plots (eq 39) and (b) ligand distributions in the macrospecies $[La_{4-y}Lu_y(\mathbf{L6})_3]^{12+}$ during the titration of **L6** with La(III) and Lu(III) ($y = 0-4$, total ligand concentration $= 10^{-2}$ M, total metal concentration $= 1.33 \times 10^{-2}$ M, lanthane mole fractions $x_{La} = |La|/(|La| + |Lu|) = 0-1$).

the successive introduction of La(III) is less anti-cooperative (even slightly positively cooperative for $0 \leq r^{La}_{(L6)3} \leq 2$) than the same process with Lu(III), and therefore the $[La_3Lu(\mathbf{L6})_3]^{12+}$ macrospecies dominates the related $[LaLu_3(\mathbf{L6})_3]^{12+}$ macrospecies during the titration. This unsymmetrical situation drastically differs from the non-cooperative case characterized by $\Delta E^{mix}_{1-2} = 0$, for which the Scatchard-like plots are linear (part a of Figure S4, Supporting Information), and the distribution curves do not show preferences for a specific heterobimetallic macrospecies (part b of Figure S4).

Introduction of the microscopic parameters of Table 1 for Ln = La, Lu and $\Delta E^{La,Lu}_{1-2} = 45.4$ kJ·mol^{-1} into eqs 17−26 provides the target experimental set of 10 microconstants (part a of Figure 10), which allows the calculation of the experimental distribution curves for the 10 microspecies (part b of Figure 10). The relative contributions of the different microspecies to a given macrospecies do not deviate significantly from those originally calculated in eqs 27−31 with $\Delta E^{mix}_{1-2} = 0$, which does not require further iterative fitting processes, according to the limited accuracy of the integration of the ^{1}H NMR signals. It is, however, worth noting that, when the number of La(III) metals is larger than the number of Lu(III) in a macrospecies, that is, in $[La_3Lu]$, the dominant microspecies maximizes the amount of alternance between different metals, whereas the reverse situation holds when the macrospecies contains a larger number of Lu(III), that is, in $[Lu_3La]$ (Figure 10).

(26) Hamacek, J.; Piguet, C. *J. Phys. Chem. B* **2006**, *110*, 7783−7792.

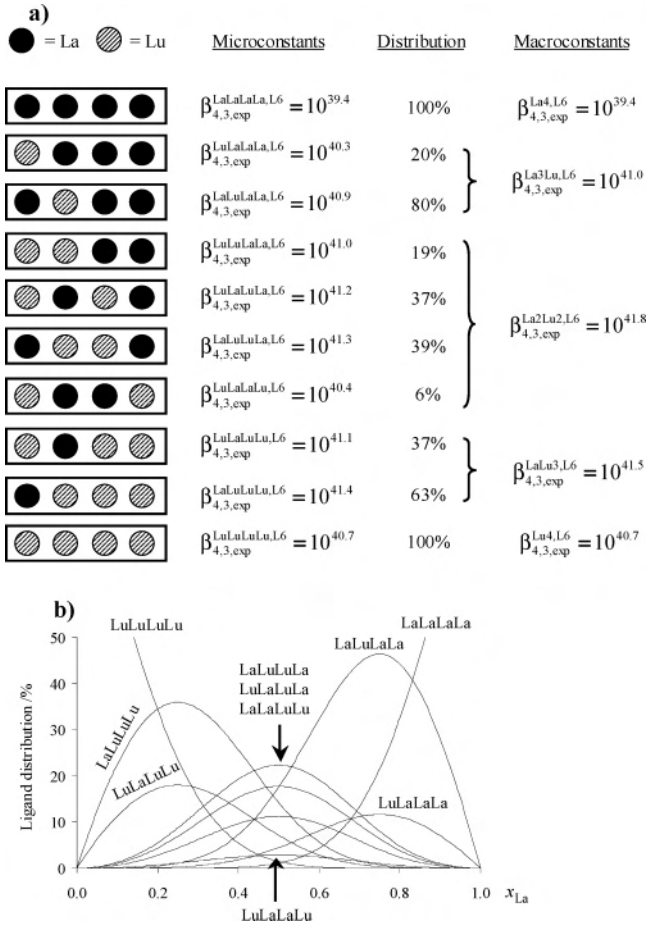

Figure 10. Experimental (a) macro- and microconstants and (b) ligand distributions in the microspecies $[La_{4-y}Lu_y(\mathbf{L6})_3]^{12+}$ during the titration of **L6** with La(III) and Lu(III) ($y = 0-4$, total ligand concentration $= 10^{-2}$ M, total metal concentration $= 1.33 \times 10^{-2}$ M, lanthane mole fractions $x_{La} = |La|/(|La| + |Lu|) = 0-1$).

Experimental Section

Chemicals were purchased from Fluka AG and Aldrich and used without further purification, unless otherwise stated. Ligand **L6** was prepared according to a literature procedure.[23] $Ln(CF_3SO_3)_3{\cdot}xH_2O$ (Ln = La, Lu)[27] were prepared from the corresponding oxides (Aldrich, 99.99%). The lanthanide content of solid salts was determined by complexometric titrations with Titriplex III (Merck) in the presence of urotropine and xylene orange.[28] Acetonitrile and dichloromethane were distilled over calcium hydride.

Spectroscopic and Analytical Measurements. ^{1}H NMR spectra were recorded at 25 °C on Bruker Avance 400 MHz and Bruker DRX-500 MHz spectrometers. Chemical shifts are given in ppm with respect to TMS. The samples for ^{1}H NMR spectroscopy were prepared by the stoichiometric 3:4 mixing of **L6** and $Ln(CF_3SO_3)_3{\cdot}xH_2O$ (Ln = La, Lu) in 700 μL of CD_3CN/CD_2Cl_2 (95:5). The total concentration of the ligand was maintained at 10 mM in each sample and 48 h equilibration was required before measurements. Because of partial overlap in the proton spectrum, signal amplitudes were determined by line-shape analysis followed by spectral reconstruction using the Bruker's Winnmr deconvolution tool. Computations of the concentrations were performed with the HySS2

(27) Desreux, J. F. In *Lanthanide Probes in Life, Chemical and Earth Sciences*; Bünzli, J.-C. G., Choppin, G. R., Eds.; Elsevier Science: Amsterdam, The Netherlands, 1989; Chap. 2.

(28) Schwarzenbach, G. *Complexometric Titrations*; Chapman & Hall: London, 1957 p. 8.

program (Protonic software). Least-squares fitting methods were implemented in Excel and Mathematica.

Conclusion

Better understanding of the thermodynamic driving forces controlling multicomponent self-assembly processes opens novel perspectives for addressing the unsolved chemical challenge of selectively introducing different lanthanides possessing very similar coordination properties, but slightly different sizes, into organized linear polymetallic chains. According to the present results, the stepwise increasing length of the ligand strands, and consequently of the number of successive binding sites, produces an anti-cooperative process, which favors the alternance of lanthanides of different sizes along the helical axis (part b of Figure 3). For the investigated La(III)/Lu(III) pair, the minor deviation from the mixing rule $\Delta E_{1-2}^{\mathrm{mix}} = (\Delta E_{1-2}^{\mathrm{Lu,Lu}} + \Delta E_{1-2}^{\mathrm{La,La}})/2 - \Delta E_{1-2}^{\mathrm{La,Lu}} \approx 2\ \mathrm{kJ \cdot mol^{-1}}$ indeed agrees with the minor changes occurring between La(III) and Lu(III), but it becomes significant for the tetranuclear helicates $[La_4(\mathbf{L6})_3]^{12+}$ because of its amplification by the repetition of this specific effect in polynuclear complexes. Because mechanical coupling is limited to short-range interactions, we can conclude that solvation effects and electrostatic interactions, which operate on large nanometric scales, are mainly responsible for this unprecedented segregation. Although we are still not in a position to chemically control this effect, we have succeeded to find a case where $\Delta E_{1-2}^{\mathrm{mix}} \neq 0$ for which we predict a particularly attractive application in the prospection of bifunctional sensors[7] and directional energy transfer processes[4,5] and the development of four-level molecular lasers.[29] With this novel tool at hand, the next step for addressing the heterometallic 4f−4f challenge involves the design of novel systems displaying $|\Delta E_{1-2}^{\mathrm{mix}}| \gg RT$ and for which a robust thermodynamic organization of the metals occurs along the ligand strands.

Acknowledgment. Financial support from the COST D31 action and from the Swiss National Science Foundation is gratefully acknowledged.

Supporting Information Available: Tables (S1−S5) and Figures (S1−S4) corresponding to thermodynamic and structural modeling, spectroscopic analyses, and fitting processes. This material is available free of charge via the Internet at http://pubs.acs.org.

IC701308H

(29) Reisfeld, R.; Jørgensen, C. K. *Lasers and Excited States of Rare Earths, Inorganic Chemistry Concepts*; Springer-Verlag: Heidelberg, Germany, 1977; Vol. 1, pp 76−79.